
Uncertainty-aware Accumulated Local Effects (UALE) for quantifying the heterogeneity of instance-level feature effects

Anonymous Author
Anonymous Institution

Abstract

Accumulated Local Effects (ALE) is a popular explainable AI method that quantifies how a feature influences the decisions of a model, handling well feature correlations. In case of complex interactions between features, instance-level feature effects may deviate from the ALE curve. It is therefore crucial to quantify this deviation, namely, the uncertainty of the effect. In this work, we define Uncertainty-aware ALE (UALE) to quantify and visualize, on a single plot, both the average effect and its uncertainty. We show that UALE quantifies uncertainty effectively, even in case of correlated features. We also note that as in ALE, UALE’s approximation requires partitioning the feature domain into non-overlapping intervals (bin-splitting). The average effect and the uncertainty are computed from the instances that lie in each bin. We formally prove that to achieve an unbiased approximation of the uncertainty in each bin, bin-splitting must follow specific constraints. Based on this, we propose a method to determine the optimal intervals, [balancing the estimation bias and variance.] We demonstrate, through synthetic and real datasets, (a) the advantages of modeling the uncertainty with UALE compared to alternative methods and (b) the effectiveness of UALE’s appropriate bin splitting for a [good] approximating of the average effect and its uncertainty.

1 INTRODUCTION

Recently, Machine Learning (ML) has been widely adopted in mission critical domains, such as healthcare and finance. In such high-stakes areas, it is important not only to pro-

vide accurate predictions but also meaningful explanations. For this reason, there is an increased interest in Explainable AI (XAI). XAI literature distinguishes between local and global methods (Molnar et al., 2020a). Local methods provide instance-level explanations, i.e., explain the prediction for a specific instance, whereas global methods summarize the entire model behavior. Global methods create a global explanation by aggregating the instance-level explanations into a single interpretable outcome, usually a number or a plot.

A popular class of global XAI are feature effect (FE) methods (Grömping, 2020) that quantify the average (over all instances) effect of a single feature on the output¹. There are three widely-used FE methods: *Partial Dependence Plots* (PDP)(Friedman, 2001), *Marginal Plots* (MP)(Apley and Zhu, 2020) and *Accumulated Local Effects* (ALE)(Apley and Zhu, 2020). ALE is established as the state-of-the-art in quantifying the average effect, since PDP and MP have been criticized (Grömping, 2020) of providing misleading explanations in case of correlated input features.

When complex interactions between features exist, the instance-level (local) feature effects may exhibit significant deviation, aka heterogeneity, from the aggregated (global) explanation, a phenomenon known as aggregation bias (Mehrabi et al., 2021). We call this deviation *the uncertainty of the global effect*. Aggregation bias leads to ambiguities; for example, a feature with zero average effect may indicate (a) no effect on the output or (b) an effect that is highly positive for some instances and highly negative for some others. As a result, there is a need for FE methods to quantify the deviation (uncertainty) of instance-level explanations, in addition to the average effect. In the case of PDP, such deviation is visualized via the Individual Conditional Explanations (ICE) (Goldstein et al., 2015). ICE plots, however, have the same limitations as PDP in case of correlated features. No method to quantify the deviation of instance-level effects has been proposed for ALE.

In this work, we propose UALE, a global feature-effect

Preliminary work. Under review by AISTATS 2023. Do not distribute.

¹FE methods also isolate the combined effect of a pair of features to the output. Combinations of more than two features are uncommon, since they are difficult to estimate and visualize.

method that extends ALE for modeling the uncertainty of the feature effect. Our method handles well cases with correlated features. As in ALE, we provide an interval-based formulation of UALE. This formulation partitions the feature domain into non-overlapping intervals (bin-splitting) and defines the average effect (bin-effect) and its uncertainty (bin-uncertainty). We exploit this formulation to provide an UALE approximation. As we formally prove, a fixed equi-width partitioning that does not consider the characteristics of the instance-level effects, which is the case in ALE, may lead to an erroneous (biased) estimation of the uncertainty. Therefore, we propose a variable-width partitioning that leads to an unbiased approximation.

The contributions of this paper are:

- A global feature effect method (UALE) that quantifies both the average effect and its uncertainty, i.e., the deviation of instance-level effects.
- An unbiased approximation of the uncertainty through a dynamic variable-size bin partitioning of the feature domain.
- The evaluation of UALE on both synthetic and real datasets.

The implementation of our method and the code for reproducing all the experiments is provided along with the manuscript and will become publicly available upon acceptance.

2 BACKGROUND AND RELATED WORK

In the rest of the paper, we use following notation. Let $\mathcal{X} \in \mathbb{R}^d$ be the d -dimensional feature space, $\mathcal{Y} \in \mathbb{R}$ the target space and $f(\cdot) : \mathcal{X} \rightarrow \mathcal{Y}$ the black-box function. We use index $s \in \{1, \dots, d\}$ for the feature of interest and $c = \{1, \dots, d\} - s$ for the set with all other indexes. For convenience, we denote the feature vector $\mathbf{x} = (x_1, \dots, x_s, \dots, x_D)$ with (x_s, \mathbf{x}_c) and the corresponding random variables $X = (X_1, \dots, X_s, \dots, X_D)$ with (X_s, X_c) . The training set is $\mathcal{D} = \{(\mathbf{x}^i, y^i)\}_{i=1}^N$ sampled i.i.d. from the distribution $\mathbb{P}_{X,Y}$. Finally, we use $f^{\langle \text{method} \rangle}(x_s)$ for denoting the s -th FE, where $\langle \text{method} \rangle$ indicates the particular method in use, for example ALE. An extensive list with all symbols used in this paper is provided at Appendix A.

2.1 Feature Effect Methods

The three well-known feature effect methods are: *Partial Dependence Plots* (PDP), *Marginal Plots* (MP) and *Accumulated Local Effects* (ALE). PDP formulates the global FE as an expectation over the distribution of X_c ,

i.e., $f^{\text{PDP}}(x_s) = \mathbb{E}_{X_c}[f(x_s, X_c)]$, whereas MP as an expectation over the distribution of $X_c|X_s$, i.e., $f^{\text{MP}}(x_s) = \mathbb{E}_{X_c|X_s}[f(x_s, X_c)]$. Both methods suffer from misestimations in case of correlated features. PDP integrates over unrealistic instances and MP computes aggregated effects, i.e., imputes the combined effect of sets of features to a single feature (Apley and Zhu, 2020).

ALE overcomes these problems. Specifically, ALE defines the local effect of the s -th feature at a specific point (z, \mathbf{x}_c) of the input space \mathcal{X} with the partial derivative $f^s(z, \mathbf{x}_c) = \frac{\partial f}{\partial x_s}(z, \mathbf{x}_c)$. All the local explanations at z are then weighted by the conditional distribution $p(\mathbf{x}_c|z)$ and are averaged, to produce the averaged effect $\mu(z)$. ALE plot is the accumulation of the averaged local effects:

$$f^{\text{ALE}}(x_s) = \int_{x_{s,\min}}^{x_s} \underbrace{\mathbb{E}_{X_c|X_s=z}[f^s(z, X_c)]}_{\mu(z)} dz \quad (1)$$

where $x_{s,\min}$ is the minimum value of the s -th feature.

2.2 Heterogeneity Of Instance-Level Effects

The global effect is computed as an expectation over local (instance-level) effects. In addition to this global effect, it is important to know to what extent the local effects deviate from the global explanation.

ICE plots and similar methods (e.g., d-ICE plots (Goldstein et al., 2015)) provide a set of curves illustrated on top-of PDP. Each curve corresponds to one instance of the dataset, $f_i^{\text{ICE}}(x_s) = f(x_s, \mathbf{x}_c^i)$. The user then visually observes if the curves are homogeneous, i.e., all instances have similar effect plots, and to what extent they deviate from the PDP. There are methods try to automate the aforementioned visual exploration, by grouping ICE plots into clusters (Molnar et al., 2020b; Herbringer et al., 2022; Britton, 2019). Unfortunately, these methods are subject to the failure modes of PDPs in cases of correlated features (Baniecki et al., 2021), as we also confirm in our experimental analysis (c.f., Section 4.1).

Other approaches, like H-Statistic (Friedman and Popescu, 2008), Greenwell’s interaction index (Greenwell et al., 2018) or SHAP interaction values (Lundberg et al., 2018) quantify interactions between the input features. A strong interaction is an implicit indication of the existence of heterogeneous effects. These methods, however, do not quantify directly the level of heterogeneity.

To the best of our knowledge, no work exist so far that quantifies the heterogeneous effects (uncertainty) based on the formulation of ALE.

2.3 ALE Approximation

ALE is estimated from the available dataset instances. (Apley and Zhu, 2020) proposed to divide the feature domain in K bins of equal size and to estimate the local effects in each bin by evaluating the model f at the bin limits:

$$\hat{f}^{\text{ALE}}(x_s) = \sum_{k=1}^{k_x} \frac{1}{|\mathcal{S}_k|} \sum_{i: \mathbf{x}^i \in \mathcal{S}_k} [f(z_k, \mathbf{x}_c^i) - f(z_{k-1}, \mathbf{x}_c^i)] \quad (2)$$

where k_x the index of the bin that x_s belongs to, i.e. $k_x : z_{k_x-1} \leq x_s < z_{k_x}$ and \mathcal{S}_k is the set of training instances of the k -th bin, i.e. $\mathcal{S}_k = \{\mathbf{x}^i : z_{k-1} \leq x_s^i < z_k\}$. (Gkolemis et al.) proposed the Differential ALE (DALE) that computes the local effects on the training instances using auto-differentiation:

$$\hat{f}^{\text{DALE}}(x_s) = \Delta x \sum_{k=1}^{k_x} \frac{1}{|\mathcal{S}_k|} \sum_{i: \mathbf{x}^i \in \mathcal{S}_k} f^s(\mathbf{x}^i) \quad (3)$$

Their method has significant computational advantages and allows the recomputation of the accumulated effect with different bin-splitting with near-zero additional computational cost. Moreover, by avoiding the use of artificial samples at the bin limits DALE allows the use of wider bins without out-of-distribution sampling. [Maybe connect with our work]. In both cases, the approximations partition the feature domain in K equally-sized bins, without considering the underlying local effects.

3 Uncertainty-Aware ALE (UALE)

We define UALE and provide an interval-based formulation that partitions the feature domain into non-overlapping intervals (bin-splitting) and defines the bin-effect and the bin-uncertainty. Then, we present UALE approximation, formally proving the bin-splitting requirements for an unbiased estimation of the uncertainty. Based on this, we present an optimization method to determine an appropriate variable-width partitioning.

3.1 UALE Definition and Interval-Based Formulation

We quantify the uncertainty of the local effects at $x_s = z$ with the standard deviation of the local explanations, $\sigma(z)$, where:

$$\sigma^2(z) = \mathbb{E}_{X_c | X_s=z} [(f^s(z, X_c) - \mu(z))^2] \quad (4)$$

The uncertainty emerges from (a) the feature correlations and (b) the implicit feature interactions of the black-box function. We also define the accumulated uncertainty at x_s , as the accumulation of the standard deviation of the local effects:

Figure 1: UALE-concept-figure

$$f_{\sigma}^{\text{ALE}}(x_s) = \int_{x_{s, \min}}^{x_s} \sigma(z) \partial z \quad (5)$$

UALE defines the effect as a pair that consists of the average effect and the uncertainty $(\mu(z), \sigma(z))$. For visualizing it, we use the accumulated average effect, as defined in Eq. (1), and the accumulated uncertainty, as defined in Eq. (5). Figure 1 illustrates an example [Describe after putting the figure].

For the interval-based formulation, we define the bin-effect $\mu(z_1, z_2)$ and the bin-uncertainty $\sigma(z_1, z_2)$ as:

$$\mu(z_1, z_2) = \mathbb{E}_{z \sim \mathcal{U}(z_1, z_2)} [\mu(z)] = \frac{\int_{z_1}^{z_2} \mu(z) \partial z}{z_2 - z_1} \quad (6)$$

$$\sigma^2(z_1, z_2) = \mathbb{E}_{z \sim \mathcal{U}(z_1, z_2)} [\sigma^2(z)] = \frac{\int_{z_1}^{z_2} \sigma^2(z) \partial z}{z_2 - z_1} \quad (7)$$

Intuitively, if we randomly draw a point z^* from a uniform distribution $z^* \sim \mathcal{U}(z_1, z_2)$, the bin-effect (Eq. (6)) and the bin-uncertainty (Eq. (7)) are the expected average effect and the expected uncertainty, respectively. Also, if we denote as \mathcal{Z} the sequence of $K + 1$ points that partition the domain of the s -th feature into K variable-size intervals, i.e. $\mathcal{Z} = \{z_0, \dots, z_K\}$, we provide the interval-based formulation of UALE:

$$\hat{f}_{\mathcal{Z}, \mu}^{\text{ALE}}(x_s) = \sum_{k=1}^{k_x} \mu(z_{k-1}, z_k) (z_k - z_{k-1}) \quad (8)$$

$$\hat{f}_{\mathcal{Z}, \sigma}^{\text{ALE}}(x_s) = \sum_{k=1}^{k_x} \sigma(z_{k-1}, z_k) (z_k - z_{k-1}) \quad (9)$$

where k_x is the index of the bin such that $z_{k_x-1} \leq x_s < z_{k_x}$. Eq. (8) and Eq. (9) are piecewise-linear approximation of Eq. (1) and Eq. (5).

3.2 UALE Interval-Based Approximation

For approximating the bin-effect and the bin-uncertainty, we use the set \mathcal{S}_k of dataset instances with the s -th feature lying inside the k -th bin, i.e., $\mathcal{S}_k = \{\mathbf{x}^i : z_{k-1} \leq x_s^i < z_k\}$. The bin-effect is approximated with,

$$\hat{\mu}(z_{k-1}, z_k) = \frac{1}{|\mathcal{S}_k|} \sum_{i: \mathbf{x}^i \in \mathcal{S}_k} [f^s(\mathbf{x}^i)] \quad (10)$$

which is an unbiased estimator of Eq. (6) under the assumption that the points are uniformly distributed inside the interval. The approximation for the uncertainty (Eq. (7)) from the available instances is defined as follows:

$$\hat{\sigma}^2(z_{k-1}, z_k) = \frac{1}{|S_k|} \sum_{i: \mathbf{x}^i \in S_k} (f^s(\mathbf{x}^i) - \hat{\mu}(z_1, z_2))^2 \quad (11)$$

In the Appendix B, we show that $\hat{\sigma}^2(z_1, z_2)$ is an unbiased estimator of $\sigma_*^2(z_1, z_2) = \frac{\int_{z_1}^{z_2} \mathbb{E}_{X_c|X_s=z} [(f^s(z, X_c) - \mu(z_1, z_2))^2] dz}{z_2 - z_1}$. In Theorem 3.1 we prove that in the general case, $\sigma_*^2(z_1, z_2) \geq \sigma^2(z_1, z_2)$, so $\hat{\sigma}^2(z_1, z_2)$ is an overestimation of the bin uncertainty.

Theorem 3.1. *If we define (a) the residual $\rho(z)$ as the difference between the expected effect at z and the bin-effect, i.e. $\rho(z) = \mu(z) - \mu(z_1, z_2)$ and (b) $\mathcal{E}(z_1, z_2)$ as the mean squared residual of the bin, i.e. $\mathcal{E}(z_1, z_2) = \frac{\int_{z_1}^{z_2} \rho^2(z) dz}{z_2 - z_1}$, then it holds*

$$\sigma_*^2(z_1, z_2) = \sigma^2(z_1, z_2) + \mathcal{E}(z_1, z_2) \quad (12)$$

Proof. The proof is at Appendix C. \square

We refer to $\mathcal{E}^2(z_1, z_2)$ as bin-error. Based on Theorem 3.1, the estimation is unbiased only when $\mathcal{E}^2(z_1, z_2) = 0$.

3.3 Bin-Splitting

The quality of UALE approximation is affected by (a) the population of samples in each bin and (b) the error term $\mathcal{E}(z_1, z_2)$ of each bin. On the one hand, we favor a partitioning of the feature domain in large-bins to allow a robust estimation of $\hat{\mu}(z_1, z_2)$, $\hat{\sigma}(z_1, z_2)$ from a sufficient population of samples. On the other hand, we want to minimize the cumulative bin-error, i.e., $\mathcal{E}_Z^2 = \sum_{k=1}^K \mathcal{E}^2(z_1, z_2) \Delta z_k$, where $Z = \{z_0, \dots, z_K\}$ and $\Delta z_k = z_k - z_{k-1}$. We search for a partitioning that balances this trade-off.

Corollary 3.1.1 shows that minimizing \mathcal{E}_Z^2 is equivalent to minimizing $\sum_{k=1}^K \sigma_*^2(z_{k-1}, z_k) \Delta z_k$, which can be directly estimated from $\sum_{k=1}^K \hat{\sigma}^2(z_{k-1}, z_k) \Delta z_k$.

Corollary 3.1.1. *A bin-splitting Z that minimizes the accumulated error if and only if it also minimizes $\sum_{k=1}^K \sigma_*^2(z_1, z_2) \Delta z_k$*

Proof. The proof is based on the observation that $\sum_{k=1}^K \sigma^2(z_{k-1}, z_k) \Delta z_k = \sigma^2(z_0, z_K)(z_K - z_0)$ which is independent of the bin-splitting. A more detailed proof is provided in the Appendix D. \square

Based on the above, we set-up the following optimization problem:

$$\begin{aligned} \min_{Z=\{z_0, \dots, z_K\}} \quad & \mathcal{L} = \sum_{k=1}^K \tau_k \hat{\sigma}^2(z_{k-1}, z_k) \Delta z_k \\ \text{where} \quad & \Delta z_k = z_k - z_{k-1} \\ & \tau_k = 1 - \alpha \frac{|S_k|}{N} \\ \text{s.t.} \quad & |S_k| \geq N_{\text{PPB}} \\ & z_0 = x_{s, \min} \\ & z_K = x_{s, \max} \end{aligned} \quad (13)$$

The objective \mathcal{L} searches for a partitioning $Z_* = \{z_0, \dots, z_K\}$ with low aggregated error \mathcal{E}_Z^2 . In case of many partitionings with similar aggregate-error, the term τ_k favors the partitioning with more points per bin, i.e., with wider bins. The constraint of at least N_{PPB} points per bin sets the lowest-limit for a *robust* estimation. The user can choose to what extent they favor the creation of wide bins through (a) the parameter α that controls the discount τ_k and (b) the parameter N_{PPB} that sets the minimum population per bin. For providing a rough idea, in our experiments we set $\alpha = 0.2$ which means that the discount ranges between $[0\%, 20\%]$ and $N_{\text{PPB}} = \frac{N}{20}$, where N is the dataset size.

For solving the optimization problem of Eq.13 we add some constraints. First, we set a threshold K_{\max} on the maximum number of bins which, in turn, defines the minimum bin-width, i.e. $\Delta x_{\min} = \frac{x_{s, \max} - x_{s, \min}}{K_{\max}}$. Based on that, we restrict the bin-limits to the multiples of the minimum width, i.e. $z_k = k \cdot \Delta x_{\min}$, where $k \in \{0, \dots, K_{\max}\}$. In this discretized solution space, we find the global optimum using dynamic programming. [Add description] See also Appendix E.

4 SIMULATION EXAMPLES

Similarly to (Aas et al., 2021; Herbringer et al., 2022) we first use simulation examples for evaluation. The first group (Section 4.1) compares UALE against PDP-ICE in modeling the average effect and the uncertainty. The second group (Section 4.2) compares UALE approximation with optimal bin-splitting against the fixed-size alternative.

4.1 Case 1: UALE vs PDP-ICE

The aim of this example is to highlight that when features are correlated, PDP and ICE fail in quantifying the average effect and the heterogeneity, even when the black-box function is relatively simple.

We use the following distribution: $p(\mathbf{x}) = p(x_3)p(x_2|x_1)p(x_1)$ where $x_1 \sim \mathcal{U}(0, 1)$, $x_2 = x_1$ and $x_3 \sim \mathcal{N}(0, \sigma_3^2)$ and the following piecewise linear function:

$$f(\mathbf{x}) = \begin{cases} f_1(\mathbf{x}) + \alpha f_2(\mathbf{x}) & \text{if } f_1(\mathbf{x}) < \frac{1}{2} \\ \frac{1}{2} - f_1(\mathbf{x}) + \alpha f_2(\mathbf{x}) & \text{if } \frac{1}{2} \leq f_2(\mathbf{x}) < 1 \\ \alpha f_1(\mathbf{x}) & \text{otherwise} \end{cases} \quad (14)$$

where $f_1(\mathbf{x}) = a_1x_1 + a_2x_2$ and $f_2(\mathbf{x}) = x_1x_3$. The linear term f_1 includes the two correlated features and the interaction term f_2 the two non-correlated. We evaluate the effect computed by UALE and PDP-ICE in three cases; (a) without interaction ($\alpha = 0$) and equal weights ($a_1 = a_2$), (b) without interaction ($\alpha = 0$) and different weights ($a_1 \neq a_2$) and (c) with interaction ($\alpha \neq 0$) with equal weights ($a_1 = a_2$).

In all cases, we assume that because the [give ground truth effect]. We compare it against the approximations provided by each method, after generating $N = 500$ samples.

No Interaction, Equal weights. In this set-up, $\alpha = 0$ (no interaction) and the $a_1 = a_2 = 1$ (equal weights). The ground truth effect $f_\mu^{\text{GT}}(x_1)$ is: x_1 in $[0, 0.25]$, $-x_1$ in $[0.25, 0.5]$ and 0 in $[0.5, 1]$. The uncertainty is $f_{\sigma^2}^{\text{GT}}(x_1) = 0$ in $[0, 1]$ because x_1 does not interact with other variables. In Figure 2, we observe that PDP effect is wrong and ICE plots show heterogeneous effects. In contrast, UALE models correctly both the average effect and the uncertainty. Furthermore, we observe that bin-splitting is accurate (zero cumulative error \mathcal{E}_Z).

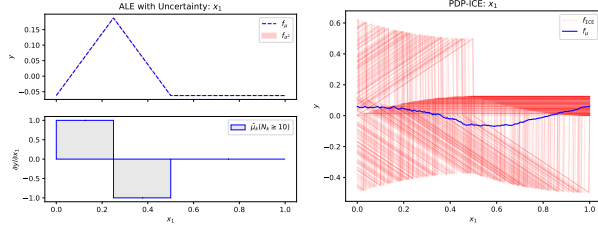


Figure 2: No interaction, Equal weights: Feature effect for x_1 using UALE (Left) and PDP-ICE (Right).

No Interaction, Non-Equal Weights. In this set-up, $\alpha = 0$ (no interaction), $a_1 = 2$ and $a_2 = 0.5$ (non-equal weights). The non-equal weights have implications at both the gradient and the interval of the piece-wise linear regions, i.e., $f_\mu^{\text{GT}}(x_1)$ is: $2x_1$ in $[0, 0.2]$, $-2x_1$ in $[0.2, 0.4]$ and 0 in $[0.4, 1]$. As before, the ground-truth uncertainty is $f_{\sigma^2}^{\text{GT}}(x_1) = 0$ because x_1 does not interact with other features. In Figure 3, we observe that PDP estimation is opposite to the ground-truth effect, i.e. negative in the region $[0, 0.2)$, positive in $[0.2, 0.4)$, and the ICE erroneously implies the existence of heterogeneous effects. As before, ALE quantifies correctly the ground truth effect, the zero-uncertainty and partitioning correctly the x_1 domain.

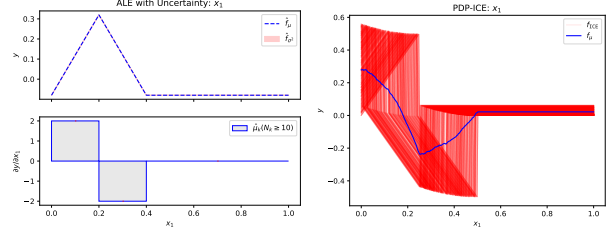


Figure 3: No interaction, Different weights: Feature effect for x_1 using UALE (Left) and PDP-ICE (Right).

With Interaction, Equal weights. In this set-up, we activate the interaction term, i.e. $\alpha = 1$, keeping the weights equal $a_1 = a_2 = 1$. The interaction term provokes heterogeneous effects for features x_1 and x_3 , because the local effects at x_1 depend on the unknown value of x_3 and vice-versa. The effect of x_2 has zero-uncertainty since it does not appear in any interaction term. As we observe in Figure 4, UALE correctly models the average effect and the uncertainty in all cases. On the other hand, PDP-ICE quantifies correctly the average effect and the uncertainty only in the case of feature x_3 , because it is independent from other features. For the correlated features x_1 and x_2 both the average effect (PDP) and the uncertainty (ICE) are wrong.

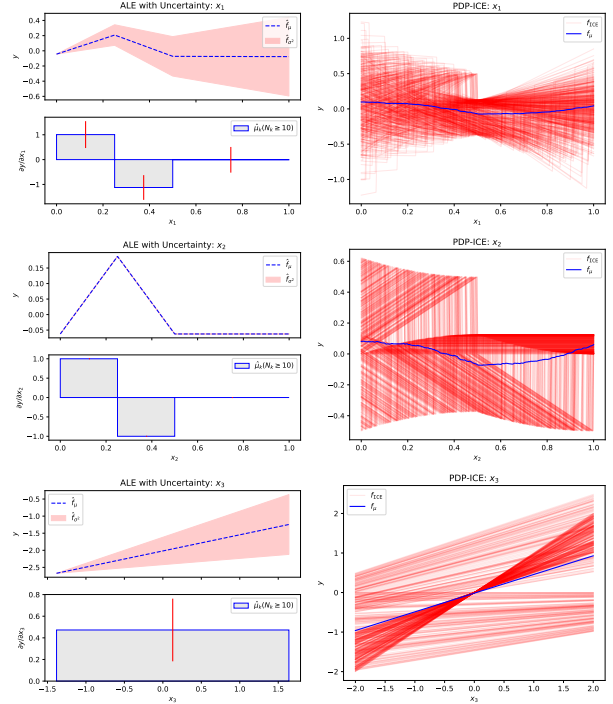


Figure 4: With interaction, equal weights: From top to bottom, feature effect for features $\{x_1, x_2, x_3\}$ using UALE (left column) and PDP-ICE (right column).

Discussion. Despite the model’s simplicity, PDP-ICE fail in modeling both the average effect and the uncertainty. The error is due to the method’s formulation, i.e. the use of the marginal distribution that ignores correlations between features, and not due to poor approximation because of limited samples. In contrast, UALE models both correctly and estimates them accurately using an optimal bin splitting in terms of Eq. (13). The examples above do not cover the case of an interaction term between correlated features, for example a term x_1x_2 , because there is an open debate about the ground-truth effect in this case (Grömping, 2020).

4.2 Case 2: Bin-Splitting

In this simulation, we illustrate the advantages of automatic bin-splitting against the fixed-size alternative. For this reason, we generate a very big dataset applying dense sampling ($N = 10^6$) and we treat the estimation with dense fixed-size bins ($K = 10^3$) as the ground-truth UALE. Afterwards, we generate fewer samples ($N = 500$) and we compare the fixed-size estimation (for several K) against UALE automatic bin-splitting. In all set-ups, we sample from $p(\mathbf{x}) = p(x_2|x_1)p(x_1)$ where $x_1 \sim \mathcal{U}(0, 1)$ and $x_2 \sim \mathcal{N}(x_1, \sigma_2^2 = 0.5)$. We denote as $\mathcal{Z}^* = \{z_0^*, \dots, z_K^*\}$ the sequence obtained by automatic bin-splitting and with \mathcal{Z}^K the fixed-size splitting with K bins. The evaluation metrics we report are the average number of independent runs $t = 30$, using each time $N = 500$ different samples.

Metrics Evaluation is perform in terms of the Mean Absolute Error (MAE) of the estimation of μ and σ across bins, i.e.,

$$\mathcal{L}^\mu = \frac{1}{|\mathcal{Z}|} \sum_{k \in \mathcal{Z}} |\mu(z_{k-1}, z_k) - \hat{\mu}(z_{k-1}, z_k)| \quad (15)$$

$$\mathcal{L}^\sigma = \frac{1}{|\mathcal{Z}|} \sum_{k \in \mathcal{Z}} |\sigma(z_{k-1}, z_k) - \hat{\sigma}(z_{k-1}, z_k)| \quad (16)$$

The ground truth UALE is the average of the dense fixed-size bins that are within in the interval $[z_{k-1}, z_k]$. For better interpretation of \mathcal{L}^σ , we also provide the mean error term $\mathcal{L}^\rho = \frac{1}{|\mathcal{Z}|} \sum_{k \in \mathcal{Z}} \mathcal{E}(z_{k-1}, z_k)$.

Piecewise-Linear Function. In this set-up, $f(\mathbf{x}) = a_1x_1 + x_1x_2$ is a piecewise-linear function with 5 different-width regions, i.e., a_1 equals to $\{2, -2, 5, -10, 0.5\}$ in the intervals defined by the sequence $\{0, 0.2, 0.4, 0.45, 0.5, 1\}$.

As we observe in the top left of Figure 5, UALE’s bin-splitting separates the fine-grained bins, e.g. regions $[0.4, 0.45]$, $[0.45, 0.5]$, and unites (most) constant-effect regions into a single bin, e.g. region $[0.5, 1]$. This explains the fact that UALE achieves lower MAE \mathcal{L}^μ , \mathcal{L}^σ compared to fixed-size bins for all K .

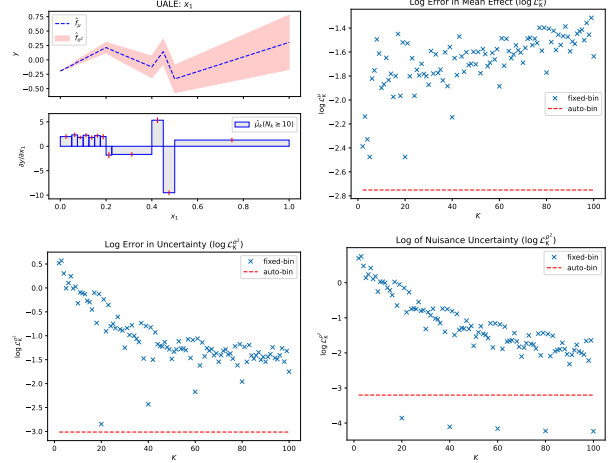


Figure 5: Figure 1

Non-Linear Function. In this set-up, $f(\mathbf{x}) = 4x_1^2 + x_2^2 + x_1x_2$, so the effect is non-linear in $0 \leq x_1 \leq 1$. Due to this non-linearity, wide bins increase \mathcal{L}^ρ making the uncertainty approximation biased. On the other hand, narrow bins lead to worse approximation due to the limited number of samples. Interestingly, in Figure 6, we observe that UALE’s bin splitting manages to compromise these conflicting objectives.

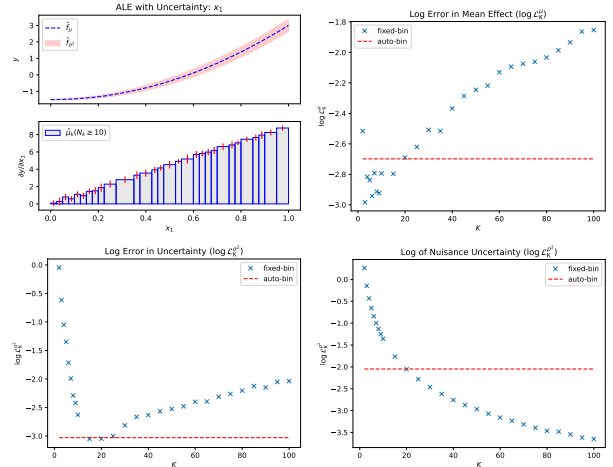


Figure 6: Figure 1

5 REAL-WORLD EXAMPLE

Here, we aim at demonstrating the usefulness of uncertainty quantification and the advantages of UALE’s approximation, on the real-world California Housing dataset (Pace and Barry, 1997).

ML setup The California Housing is a largely-studied dataset with approximately 20000 training instances, mak-

ing it appropriate for robust approximation with large K . The dataset contains $D = 8$ numerical features with characteristics about the building blocks of California, e.g. latitude, longitude, population of the block or median age of houses in the block. The target variable is the median value of the houses inside the block in dollars that ranges between $[15, 500] \cdot 10^3$, with a mean value of $\mu_Y \approx 201 \cdot 10^3$ and a standard deviation of $\sigma_Y \approx 110 \cdot 10^3$.

We exclude instances with missing and outlier values. As outlier we define the feature values which are over three standard deviations away from the mean feature value. We also normalize all features to zero-mean and unit standard deviation. We split the dataset into $N_{tr} = 15639$ training and $N_{test} = 3910$ test examples (80/20 split) and we fit a Neural Network with 3 hidden layers of 256, 128 and 36 units respectively. After 15 epochs using the Adam optimizer with learning rate $\eta = 0.02$, the model achieves a MAE of $37 \cdot 10^3$ dollars.

Below, we illustrate the feature effect for three features: latitude x_2 , population x_6 and median income x_8 . The particular features cover the main FE cases, e.g. positive/negative trend and linear/non-linear curve, and are therefore appropriate for illustration purposes. Results for all features, along with in-depth information about the preprocessing, training and evaluation parts are provided in the Appendix.

Uncertainty Quantification In real-world datasets, it is infeasible to obtain the ground truth FE for evaluation. We observe in Figure 7 that in broad terms UALE and PDP-ICE plots agree on the average effect and the uncertainty. It is interesting to note that UALE has selected bins of varying size as the optimal partitioning. This demonstrates an important advantage of UALE; through the bin splitting process we can identify wide intervals of the feature domain with similar level of uncertainty.

Bin Splitting We evaluate the robustness of UALE approximation. Following the evaluation framework of Section 4.2, we treat as ground-truth the effects computed on the full training-set $N = 20000$ with dense fixed-size bin-splitting ($K = 80$). Given the big number of samples, we make the hypothesis that the approximation with dense binning is close to the ground truth. Afterwards, we randomly select fewer samples, $N = 1000$, and we compare UALE approximation with all possible fixed-size approximation. We repeat this process $t = 30$ times. In Figure 8, we illustrate the mean values of $\mathcal{L}^\mu, \mathcal{L}^\sigma$ across the 30 repetitions. We observe that UALE achieves (near) optimal approximation in all cases. [add explanation for near-constant feature effect vs the first case that the plot]

6 DISCUSSION

[Add Conclusion, limitations, and future work]

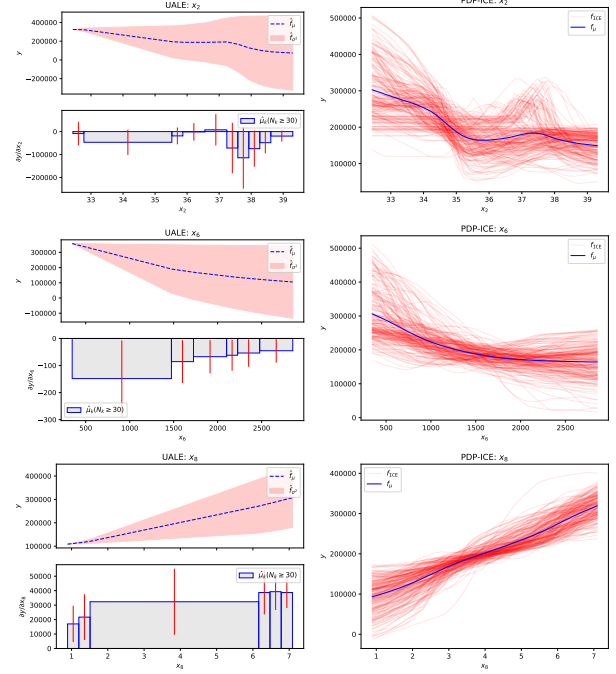


Figure 7: Figure 1

Acknowledgments

All acknowledgments go at the end of the paper, including thanks to reviewers who gave useful comments, to colleagues who contributed to the ideas, and to funding agencies and corporate sponsors that provided financial support. To preserve the anonymity, please include acknowledgments *only* in the camera-ready papers.

References

- Kjersti Aas, Martin Jullum, and Anders Løland. Explaining individual predictions when features are dependent: More accurate approximations to shapley values. *Artificial Intelligence*, 298:103502, 2021.
- Daniel W Apley and Jingyu Zhu. Visualizing the effects of predictor variables in black box supervised learning models. *Journal of the Royal Statistical Society: Series B (Statistical Methodology)*, 82(4):1059–1086, 2020.
- Hubert Baniecki, Wojciech Kretowicz, and Przemyslaw Biecek. Fooling partial dependence via data poisoning. *arXiv preprint arXiv:2105.12837*, 2021.
- Matthew Britton. Vine: visualizing statistical interactions in black box models. *arXiv preprint arXiv:1904.00561*, 2019.
- Jerome H Friedman. Greedy function approximation: a gradient boosting machine. *Annals of statistics*, pages 1189–1232, 2001.
- Jerome H Friedman and Bogdan E Popescu. Predictive

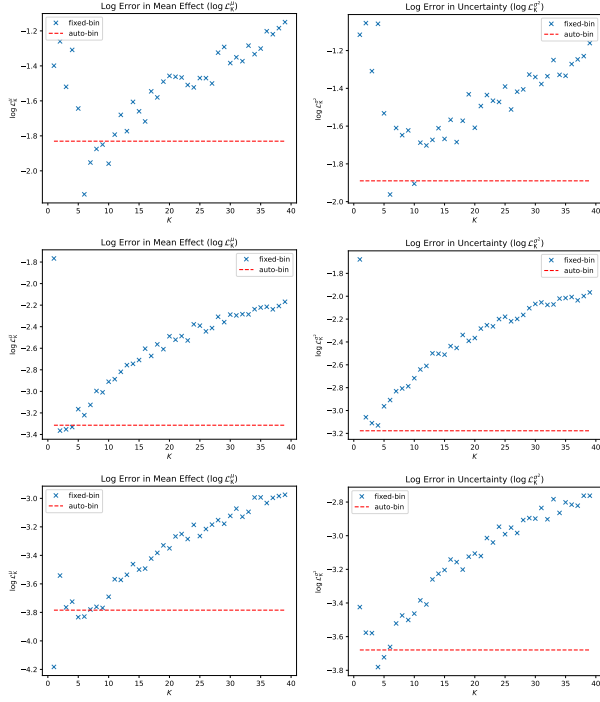


Figure 8: Figure 1

learning via rule ensembles. *The annals of applied statistics*, pages 916–954, 2008.

Vasilis Gkolemis, Theodore Dalamagas, and Christos Diou. Dale: Differential accumulated local effects for efficient and accurate global explanations.

Alex Goldstein, Adam Kapelner, Justin Bleich, and Emil Pitkin. Peeking inside the black box: Visualizing statistical learning with plots of individual conditional expectation. *journal of Computational and Graphical Statistics*, 24(1):44–65, 2015.

Brandon M Greenwell, Bradley C Boehmke, and Andrew J McCarthy. A simple and effective model-based variable importance measure. *arXiv preprint arXiv:1805.04755*, 2018.

Ulrike Grömping. Model-agnostic effects plots for interpreting machine learning models, 03 2020.

Julia Herbringer, Bernd Bischl, and Giuseppe Casalicchio. Repid: Regional effect plots with implicit interaction detection. In *International Conference on Artificial Intelligence and Statistics*, pages 10209–10233. PMLR, 2022.

Scott M Lundberg, Gabriel G Erion, and Su-In Lee. Consistent individualized feature attribution for tree ensembles. *arXiv preprint arXiv:1802.03888*, 2018.

Ninareh Mehrabi, Fred Morstatter, Nripsuta Saxena, Kristina Lerman, and Aram Galstyan. A survey on bias and fairness in machine learning. *ACM Computing Surveys (CSUR)*, 54(6):1–35, 2021.

Christoph Molnar. *Interpretable Machine Learning*. 2 edition, 2022. URL <https://christophm.github.io/interpretable-ml-book>.

Christoph Molnar, Giuseppe Casalicchio, and Bernd Bischl. Interpretable machine learning—a brief history, state-of-the-art and challenges. In *Joint European Conference on Machine Learning and Knowledge Discovery in Databases*, pages 417–431. Springer, 2020a.

Christoph Molnar, Gunnar König, Bernd Bischl, and Giuseppe Casalicchio. Model-agnostic feature importance and effects with dependent features—a conditional subgroup approach. *arXiv preprint arXiv:2006.04628*, 2020b.

R Kelley Pace and Ronald Barry. Sparse spatial autoregressions. *Statistics & Probability Letters*, 33(3):291–297, 1997.

A List with Symbols

B Show that is unbiased estimator

C Proof of Theorem 3.1

D Proof of Corollary 3.3

E Dynamic Programming

[Review all the description] For achieving a computationally-grounded solution we set a threshold K_{max} on the maximum number of bins which also discretizes the solution space. The width of the bin can take discrete values that are multiple of the minimum step $u = \frac{x_{s,max} - x_{s,min}}{K_{max}}$. For defining the solution, we use two indexes. The index $i \in \{0, \dots, K_{max}\}$ denotes the point (z_i) and the index $j \in \{0, \dots, K_{max}\}$ denotes the position of the j -th multiple of the minimum step, i.e., $x_j = x_{s,min} + j \cdot u$. The recursive cost function $T(i, j)$ is the cost of setting $z_i = x_j$:

$$T(i, j) = \min_{l \in \{0, \dots, K_{max}\}} [\mathcal{T}(i-1, l) + \mathcal{B}(x_l, x_j)] \quad (17)$$

where $\mathcal{T}(0, j)$ equals zero if $j = 0$ and ∞ in any other case. $\mathcal{B}(x_l, x_j)$ denotes the cost of creating a bin with limits $[x_l, x_j]$:

$$\mathcal{B}(x_l, x_j) = \begin{cases} \infty, & \text{if } x_j > x_l \text{ or } |\mathcal{S}(x_j, x_l)| < N \\ 0, & \text{if } x_j = x_l \\ \hat{\sigma}^2(x_j, x_l), & \text{if } x_j \leq x_l \end{cases} \quad (18)$$

The optimal solution is given by solving $\mathcal{L} = \mathcal{T}(K_{max}, K_{max})$ and keeping track of the sequence of steps.

- Discuss more aspects (e.g. Computational complexity)